CALL FOR PAPERS | *Cytoskeletal Networks and the Regulation of Cardiac Contractility*

Developmental changes in passive stiffness and myofilament Ca^{2+} sensitivity due to titin and troponin-I isoform switching are not critically triggered by birth

Martina Krüger,[1] Thomas Kohl,[2] and Wolfgang A. Linke[1]

[1]*Physiology and Biophysics Unit, University of Muenster, Muenster; and* [2]*German Center for Fetal Surgery and Minimally Invasive Therapy, Department of Obstetrics and Prenatal Medicine, University of Bonn, Bonn, Germany*

Krüger, Martina, Thomas Kohl, and Wolfgang A. Linke. Developmental changes in passive stiffness and myofilament Ca^{2+} sensitivity due to titin and troponin-I isoform switching are not critically triggered by birth. *Am J Physiol Heart Circ Physiol* 291: H496–H506, 2006. First published May 5, 2006; doi:10.1152/ajpheart.00114.2006.—The giant protein titin, a major contributor to myocardial mechanics, is expressed in two main cardiac isoforms: stiff N2B (3.0 MDa) and more compliant N2BA (>3.2 MDa). Fetal hearts of mice, rats, and pigs express a unique N2BA isoform (~3.7 MDa) but no N2B. Around birth the fetal N2BA titin is replaced by smaller-size N2BA isoforms and N2B, which predominates in adult hearts, stiffening their sarcomeres. Here we show that perinatal titin-isoform switching and corresponding passive stiffness (ST_p) changes do not occur in the hearts of guinea pig and sheep. In these species the shift toward "adult" proportions of N2B isoform is almost completed by midgestation. The relative contributions of titin and collagen to ST_p were estimated in force measurements on skinned cardiac muscle strips by selective titin proteolysis, leaving the collagen matrix unaffected. Titin-based ST_p contributed between 42% and 58% to total ST_p in late-fetal and adult sheep/guinea pigs and adult rats. However, only ~20% of total ST_p was titin based in late-fetal rat. Titin-borne passive tension and the proportion of titin-based ST_p generally scaled with the N2B isoform percentage. The titin isoform transitions were correlated to a switch in troponin-I (TnI) isoform expression. In rats, fetal slow skeletal TnI (ssTnI) was replaced by adult carciac TnI (cTnI) shortly after birth, thereby reducing the Ca^{2+} sensitivity of force development. In contrast, guinea pig and sheep coexpressed ssTnI and cTnI in fetal hearts, and skinned fibers from guinea pig showed almost no perinatal shift in Ca^{2+} sensitivity. We conclude that TnI-isoform and titin-isoform switching and corresponding functional changes during heart development are not initiated by birth but are genetically programmed, species-specific regulated events.

heart development; connectin; elasticity; myocardium

BIRTH IS A DRAMATIC EVENT in mammalian heart development. With the newborn's first breaths of air, the fetal circulation changes, and cardiac pump function is intensified to keep up with the increased power requirements of the newborn that suddenly lacks placental nurturing and oxygen supply. Heart rate, end-diastolic pressure, stroke volume, and left ventricular (LV) dimensions all increase to meet the metabolic demands of newborn life (4, 26). During perinatal development of myocardium, many sarcomere proteins alter their isoform pattern rather rapidly. Among them are the contractile proteins myosin heavy chain (MyHC) (9, 22, 32, 53) and α-actin (10); regulatory proteins, including troponin-I (TnI), troponin-T (TnT), tropomyosin (36, 46, 51–53), and myosin light chain-1 (60); and scaffolding proteins such as myomesin (1) and titin (27, 41, 43, 56). However, as these studies have usually been performed on altricial mammals (e.g., rats and mice) that remain nestlings until fetal development is completed a week after birth, it is not immediately obvious whether the event of birth actually is the trigger for such adaptations.

The giant polypeptide titin is one of the most abundant proteins in striated muscle cells with a huge molecular mass of 3.7 to 3.0 MDa. Titin molecules span half sarcomeres from the Z-disc to the M-line, integrate the actin and myosin filament systems, and play important roles in myofibrillar assembly, structure, and mechanics (20, 29, 42). The I-band part of the molecule harbors various elastic regions, including the so-called PEVK domain, two to three segments containing serially linked tandem-Ig-domains, and the unique N2B sequence (20, 28, 31) (Fig. 1). In mammalian hearts, titin is expressed in two principal isoforms (Fig. 1), the small and relatively stiff N2B isoform (3.0 MDa) and the larger and more compliant N2BA titin (>3.2 MDa) (13, 40). The expression ratio of N2BA to N2B, along with the content, cross-linking status, and isoform type of the major extracellular matrix (ECM) protein collagen, is a major determinant of the passive tension (PT) level in myocardium (33, 40). Alterations in titin-isoform composition are expected to have substantial effects on cardiac mechanics. Indeed, elevated N2BA:N2B isoform ratios were observed in end-stage failing hearts from patients with dilated or ischemic cardiomyopathy, and the myofibrils of these hearts exhibited lowered passive stiffness (ST_p) (33, 38, 39). A dramatic shift in cardiac titin-isoform expression and titin-based stiffness occurs during perinatal heart development of mice, rats, rabbits, and pigs (27, 41, 43, 56). Well before birth, the hearts of these species express a unique fetal N2BA isoform (~3.7 MDa) but
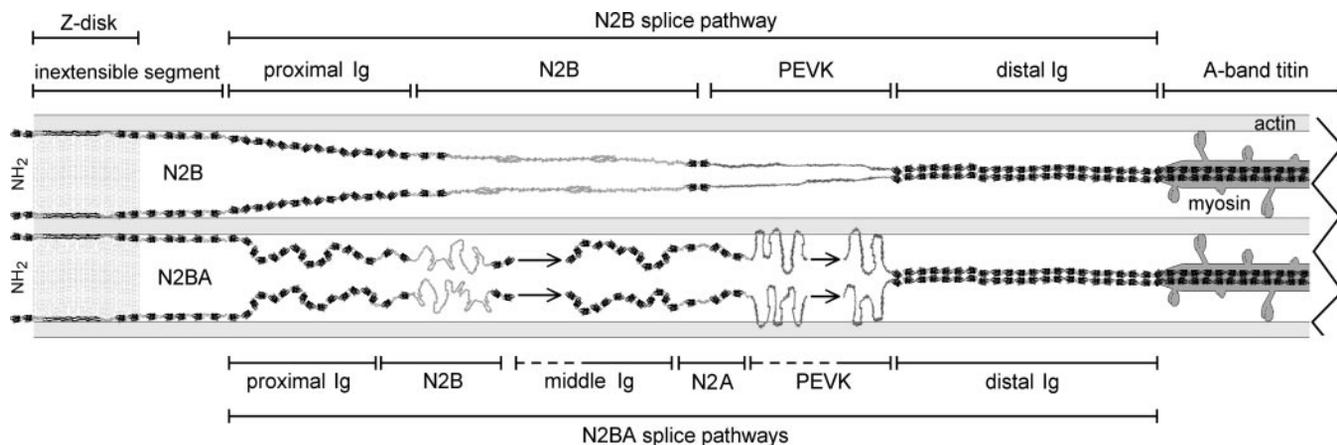

Fig. 1. Schematics of the I-band segments of the 2 principal titin isoforms, N2B and N2BA, in cardiac muscle. Structurally different regions are indicated. Size differences arise mainly from differential splicing of the middle Ig-domain region and the PEVK domain. Ig, immunoglobulin-like domain region; N2A, titin region expressed in N2BA, but not N2B, isoforms; PEVK, unique sequence rich in proline (P), glutamate (E), valine (V), and lysine (K).

no N2B isoform. Around the time of birth and shortly thereafter, this large N2BA isoform is replaced by smaller-size, less extensible N2BA isoforms and the stiff N2B isoform, which then predominates in adult hearts (27, 41, 43, 56). Consequently, the fetal or neonatal cardiac sarcomeres of these species are much more compliant than the adult sarcomeres (27, 43, 56).

In surprising contrast to these findings are earlier observations in various species suggesting that the fetal ventricle is stiffer than the mature myocardium (Ref. 44, and references therein). For instance, in sheep the ventricular compliance and distensibility increase from the fetal to the adult stage (48, 49) while during this period the myocyte volume density rises from ~40% to ~60% (54). Because ECM-based proteins, particularly collagen, greatly contribute to ST_p (27, 33, 61), it is possible that developmental changes in collagen-borne stiffness may add to alterations in myocardial compliance, either counteracting or complementing the changes in titin-based stiffness. Here we wanted to know whether perinatal changes in cardiac titin expression and mechanical function take place in guinea pig and sheep, which are nest quitters or nidifugous mammals and develop almost to the weaning stage before birth. The structural development of the hearts of these species is much advanced already by the end of the gestation period (65 days in guinea pig, ~150 days in sheep), in contrast to rats (gestation period, 22 days) (21, 54). Besides comparing the pattern of cardiac titin-isoform transitions during heart development in these three species, we also aimed at elucidating developmental changes in the relative importance of ECM structures and titin for myocardial ST_p.

The cardiac titin-isoform shift during perinatal heart development of rats closely correlates with a switch in TnI-isoform composition (56). TnI is part of the troponin complex that together with tropomyosin regulates actomyosin interaction. Like many other sarcomere proteins, TnI exists in multiple isoforms. Fetal rat hearts express a TnI isoform that is similar to the slow skeletal troponin I (ssTnI) isoform, which is replaced by a cardiac TnI (cTnI) isoform at around the time of birth (5, 7, 15, 24, 50, 52). This isoform shift is linked to a marked decrease in Ca^{2+} sensitivity of force development occurring in rats (and mice) during the postnatal period (16, 46,

53, 59). Again, the identity of the trigger(s) responsible for a coordinated isoform switching of several sarcomere proteins, including titin and TnI, has remained obscure, although available data perhaps suggested a signaling cascade that is somehow initiated by birth. Here we report that, unlike rat hearts, guinea pig and sheep hearts do not show the dramatic perinatal isoform switch of TnI and titin. The interspecies differences in isoform shifting are found to be correlated with differences in the developmental changes of ST_p and Ca^{2+} sensitivity of active force. We conclude that the developmental transitions in mechanical properties following from titin- and TnI-isoform switching are not critically triggered by the event of birth.

MATERIALS AND METHODS

Heart tissue. Heart tissue was obtained from adult pregnant Sprague-Dawley rats, fetal rats at 18 days of gestation (E18), and newborn rats 1 day after birth (each group, $n = 4$). The animals were anesthetized with ether and killed by decapitation; the complete hearts were removed, immediately frozen in liquid nitrogen, and stored at $-80°C$. Pregnant guinea pigs (adult, $n = 2$) (*Cavia aperea*), fetal animals at *day 35* (E35, $n = 2$) and *day 55* (E55, $n = 2$) of gestation, and a neonatal (1 day) guinea pig (24 h after delivery) were kindly provided by Prof. Dr. N. Sachser (Univ. of Muenster, Muenster, Germany) (25). The guinea pigs were anesthetized and killed by exsanguination, and the hearts were excised and immediately frozen in liquid nitrogen before storage at $-80°C$ until usage. Frozen heart tissue from fetal (E82, E112, E119, E135, $n = 2–3$, for each stage) and adult sheep ($n = 2$) was provided by the animal house of the University of Bonn (Germany). From all hearts we analyzed the free wall of the LVs (anterolateral-midwall region). All procedures were conducted in accordance with the guidelines of the local Animal Care and Use Committees. Protocols were approved by the Bezirksregierung Koeln (license no. 50.203.Bn_38,_28/04).

Preparation of skinned cardiac fibers. For tension measurements small muscle strips were prepared from the LVs of frozen hearts and skinned overnight in relaxing solution containing 40 μg/ml leupeptin, 30 mM 2,3-butanedione monoxime (BDM), and 0.5% wt/vol Triton X-100 on ice. The skinned tissue was extensively washed in the same buffer without Triton X-100, and small fiber bundles with diameters of 200–300 μm and a length of 1.0–2.5 mm were dissected. Dissected and skinned fibers were placed on ice in detergent-free relaxing solution and were used either for mechanical measurements or frozen

in liquid nitrogen and stored at $-80°C$ for gel electrophoresis and electron microscopy.

Mechanical measurements. Force measurements were performed with a muscle mechanics workstation (Scientific Instruments, Heidelberg, Germany) at room temperature (33, 39). Skinned LV fiber bundles were bathed in relaxing solution (7.8 mM ATP, 20 mM creatine phosphate, 20 mM imidazole, 4 mM EGTA, 12 mM Mg-proprionate, 97.6 mM K-proprionate, pH 7.0, 40 μg/ml leupeptin, 30 mM BDM) and mounted to the motor arm and force transducer between stainless steel clips. For ST_P measurements, stretch-release loops (1 Hz, 5 consecutive cycles at 5-min intervals) were performed, beginning at slack length and stretching the fibers to a maximum of 130% of their slack length (33). Sarcomere length (SL) could sometimes be detected in adult preparations by laser diffractometry (45) but not in fibers of fetal animals. However, slack SL was determined on histological (longitudinal) sections of unstretched fiber bundles or in preparations of freshly isolated myofibrillar bundles, by using a phase-contrast microscope (Zeiss Axiovert 135, ×20 objective). Fetal and adult fibers of all species had an average slack SL of 1.8–1.9 μm. Passive force was related to cross-sectional area (PT) determined from the diameter of the specimens (by assuming a cylindrical shape and circular cross-sectional area).

Titin degradation was achieved by exposing the fibers to low doses of trypsin (2 μg/ml) in relaxing buffer (without leupeptin) for up to ~1 h (30, 57). The extent of titin degradation was tested by gel electrophoresis (see below) every 10–20 min during exposure to trypsin (data not shown), and complete titin extraction was confirmed after 45–50 min of low-trypsin treatment. Passive forces were measured before and every 5 min during the titin-degradation procedure. As a measure of ST_P, we calculated the integral under the fifth stretch-release curve. ST_P was then expressed relative to the initial stiffness before addition of trypsin (33), minus the small drop in ST_P found during the ~1-h measurement period in "control" fibers not treated with trypsin, which is due to "normal" tissue softening.

To measure the Ca^{2+}-sensitivity of force development, skinned fiber bundles were mounted in relaxing solution (pCa 8.0) supplemented with 40 μg/ml leupeptin but no BDM and were prestretched by 10% of their slack length. Force-pCa relations were determined by sequentially increasing Ca^{2+} concentration to pCa 4.0. Averaged data (means ± SE) on relative-force vs. pCa diagrams were fitted by using the Hill equation. Maximum active force (=100% relative force) was usually developed at pCa 4.5.

SDS-PAGE. Tissue strips were homogenized in sample buffer containing 8 M urea, 2 M thiourea, 3% SDS (wt/vol), 75 mM DTT, 0.03% bromophenol blue, 10% glycerol, and 0.05 M Tris·HCl, pH 6.8 (57). Samples were incubated for 5 min on ice and boiled for 5 min at 95°C, followed by centrifugation. For details of sample preparation, see Refs. 39 and 43.

Conventional 10% and 15% SDS-PAGE to separate proteins in the range of 15–220 kDa was carried out according to standard protocols. For investigation of titin isoforms, agarose-strengthened SDS-PAGE with a 2% polyacrylamide concentration was performed (30, 39) by using a Laemmli buffer system and a Biometra minigel apparatus. Protein bands were visualized with Coomassie brilliant blue or by silver staining, and gels were digitized by multiple scanning by using a CanoScan 9900F scanner (Canon). Densitometry analyses were performed only on Coomassie-stained gels with the use of TotalLab software (Phoretix, Newcastle, UK). At least three gel lanes from a minimum of two hearts per developmental stage and species were analyzed, and the average titin compositions were calculated.

Immunoblotting. For Western blot analysis, protein components were separated by 15% SDS-PAGE, transferred onto a polyvinylidene difluoride membrane (Millipore, Schwalbach, Germany) by standard semidry Western blotting, and probed by monoclonal antibodies against cTnI (8I-7, Spectral Diagnostics; alternatively, H86550, BioDesign International) (39), which recognize both cTnI and ssTnI. Results were similar with the two primary antibodies. Anti-mouse

IgG-horseradish peroxidase served as secondary antibody. Enzymatic activity was detected using an ECL Kit (Amersham Biosciences, Freiburg, Germany). Attempts were made to load all lanes with equal amounts of solubilized protein after spectrophotometric analysis (Bradford method).

Histological analysis and transmission electron microscopy. LV fibers were freshly dissected from rat and guinea pig hearts and fixed in 4% paraformaldehyde (PFA). From frozen sheep heart, small muscle strips were cut and also fixed in 4% PFA. Fixed fibers were processed for histological and electron microscopic analysis according to standard protocols and were sectioned by using a Reichert ultramicrotome. Semithin (3 μm) sections of LV tissue were stained with azocarmine and aniline blue/golden orange (azan stain) to distinguish nuclei and contractile elements in the cytoplasm (red) from ECM (blue). Images were recorded with a color-CCD camera (Sony) under a Zeiss Axiovert 135 inverted microscope using 20× or 40× objectives. ECM (collagen) area density was estimated from digital images by using AxioVision LE software (Zeiss, Jena, Germany). Transmission electron micrographs of ultrathin sections were taken with a Zeiss EM 900 at 80 kV (45).

Statistics. To test for statistically significant differences, we used the unpaired Student's *t*-test. *P* values <0.05 were taken as indicating significant differences.

RESULTS

Developmental transitions in titin-isoform expression in guinea pig and sheep hearts occur already during midgestation. The proportions of the major intact-titin (T1) isoforms, N2BA and N2B, were detected by 2% SDS-PAGE in fetal, neonatal, and adult LV tissue samples from rat, guinea pig, and sheep (Fig. 2). As reported earlier for fetal rat hearts (43, 56), 4 days before birth (E18), a 3,600- to 3,700-kDa N2BA-1 isoform (60%) and a 3,500-kDa N2BA-2 isoform (30–35%) predominated, but almost no 3,000-kDa N2B titin was detectable at this developmental stage (Fig. 2, *A* and *C*). Shortly after birth (1 day), N2BA-1 titin decreased to <5%, and the proportions of N2BA-2 and N2B increased to ~40% and ~60%, respectively. Adult rat hearts expressed mainly N2B titin (>90%), whereas N2BA-1 and N2BA-2 were completely replaced by smaller-size, low-level N2BA isoforms of 3,400 kDa (N2BA-3) and 3,200 kDa (N2BA-4) (Fig. 2, *A* and *C*). The identity of the titin isoforms on the gels was confirmed by us previously by using Western blotting (43).

In fetal guinea pig hearts about halfway through the gestation period (E35), two large N2BA isoforms (3,600 kDa; 3,500 kDa) were expressed (Fig. 2*A*), each constituting 35–40% of total T1-titin, whereas N2B was still relatively scarce (25 ± 4%). In the perinatal period, 10 days before birth (E55), the proportion of N2B-titin was already ~60% (Fig. 2, *A* and *C*). Thus there is a titin-isoform switch already at relatively early developmental stages. At stage E55, at least three N2BA isoforms could be distinguished that made up ~10% [size, ~3,600 kDa ($N2BA_{3600}$)] and twice ~15% [~3,500 kDa ($N2BA_{3500}$); ~3,300 kDa ($N2BA_{3300}$)] of the total T1-titin. This isoform pattern was not significantly altered in neonatal (1 day) guinea pig hearts, which expressed ~60% N2B titin, ~5% $N2BA_{3600}$, ~20% $N2BA_{3500}$, and ~15% $N2BA_{3300}$ (Fig. 2, *A* and *C*). In adult guinea pig hearts, the two largest N2BA isoforms almost completely disappeared, but the $N2BA_{3300}$ isoform still constituted 25–30% of the T1-titin, with the remainder (~70%) representing the N2B-isoform (Fig. 2, *A* and *C*). In summary, the average N2BA:N2B
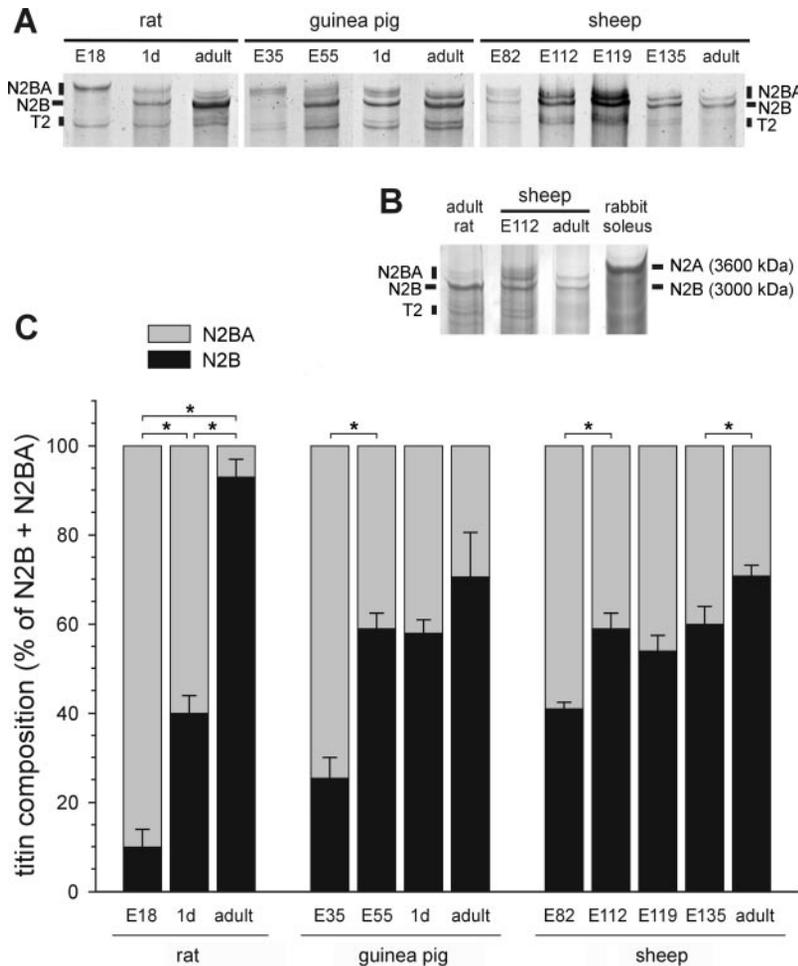
Fig. 2. Titin isoform composition in developing rat, guinea pig, and sheep left ventricle. *A*: high-resolution SDS-PAGE (2%) of tissue samples from late fetal [gestational *day 18* (E18)], neonatal [1 day (1d)] and adult rat; midgestation (E35), late-fetal (E55), neonatal (1 day), and adult guinea pig; and midgestation (E82), mid- to-late fetal (E112, E119, E135), and adult sheep. Titin isoforms N2BA and N2B, as well as the titin-degradation band, T2, are indicated. Coomassie staining. *B*: silver-stained 2% SDS-PAGE of fetal (E112) and adult sheep hearts also showing lanes loaded with adult rat heart (titin, 3,000 kDa) and adult rabbit soleus (titin, 3,600 kDa), for size comparison. *C*: mean titin-isoform compositions in the hearts of the 3 species at various developmental stages, shown as percentage of the total intact titin (N2B + N2BA isoforms). Data are means ± SE. *$P < 0.05$ in Student's *t*-test.

titin-expression ratio of guinea pig hearts changed significantly during midgestation, but not in late-fetal stages and during the perinatal period, and only little thereafter (the difference between 1 day and adult was not significant; $P > 0.05$ in Student's *t*-test).

Similar analyses of fetal and adult sheep hearts showed that also this species exhibits titin-isoform switching rather early during fetal development (Fig. 2). At midgestation (E82), fetal lamb hearts expressed at least two N2BA isoforms of ~3,600 and ~3,500 kDa, each constituting ~30% of the total titin; the remainder (~40%) was N2B isoform. Later in development, fetal lambs at stages E112, E119, and E135 (Fig. 2*A*) all expressed relatively high proportions of cardiac N2B titin, 55–60% (Fig. 2*C*). A strong N2BA band (30–35% of T1-titin) appeared at ~3,300 kDa, whereas the larger N2BA isoforms, now only faintly visible (Fig. 2, *A* and *B*), together made up the remaining 5–10%. In adult sheep heart, the low-level, larger-size N2BA isoforms disappeared, and the strong ~3,300-kDa variant remained as the only N2BA isoform (Fig. 2, *A* and *B*). The average N2BA:N2B ratio was approximately 30:70 (Fig. 2*C*). The difference in the mean N2BA:N2B ratio between fetal (E135) and adult sheep hearts was statistically significant ($P = 0.035$ in Student's *t*-test). In summary, unlike rat hearts, guinea pig and sheep hearts establish the "adult" proportions of N2B-titin isoform already well before birth.

Developmental alterations in the contribution of titin to total PT and ST_P. We wanted to know whether the importance of titin for total passive myocardial stiffness, compared with that of extramyofibrillar elements, changes from the fetal to the adult stage. A selective titin-degradation protocol (33, 61) was applied, in which skinned cardiac-fiber bundles were incubated with minute doses of trypsin for up to ~1 h and the concomitant decrease in ST_p was recorded during repeated stretch-release cycles (Fig. 3*A*) applied every 5 min. After the mechanical measurements, complete titin proteolysis was confirmed by 2% SDS-PAGE. In the gel examples shown in Fig. 4*A* (fetal E135 and adult sheep hearts), complete loss of intact titin (N2BA and N2B) is evident and the characteristic titin-degradation bands (T2 and T3) have appeared. In an attempt to test for the specificity of the mild-trypsin treatment, we studied the preservation of smaller muscle proteins with a molecular mass up to 250 kDa by 12.5% SDS-PAGE (examples for fetal E135 and adult sheep hearts are shown in Fig. 4*B*) and indeed could not detect an effect on these proteins, confirming earlier reports (33, 61). The trypsin-treated muscle strips, as well as nontreated hearts, were also investigated by electron microscopy for a possible effect on collagen, but no obvious effects on the appearance or abundance of collagen fibers were found (data not shown). The mild trypsin treatment is likely to leave the collagen fibers unaffected. The decrease in ST_p upon
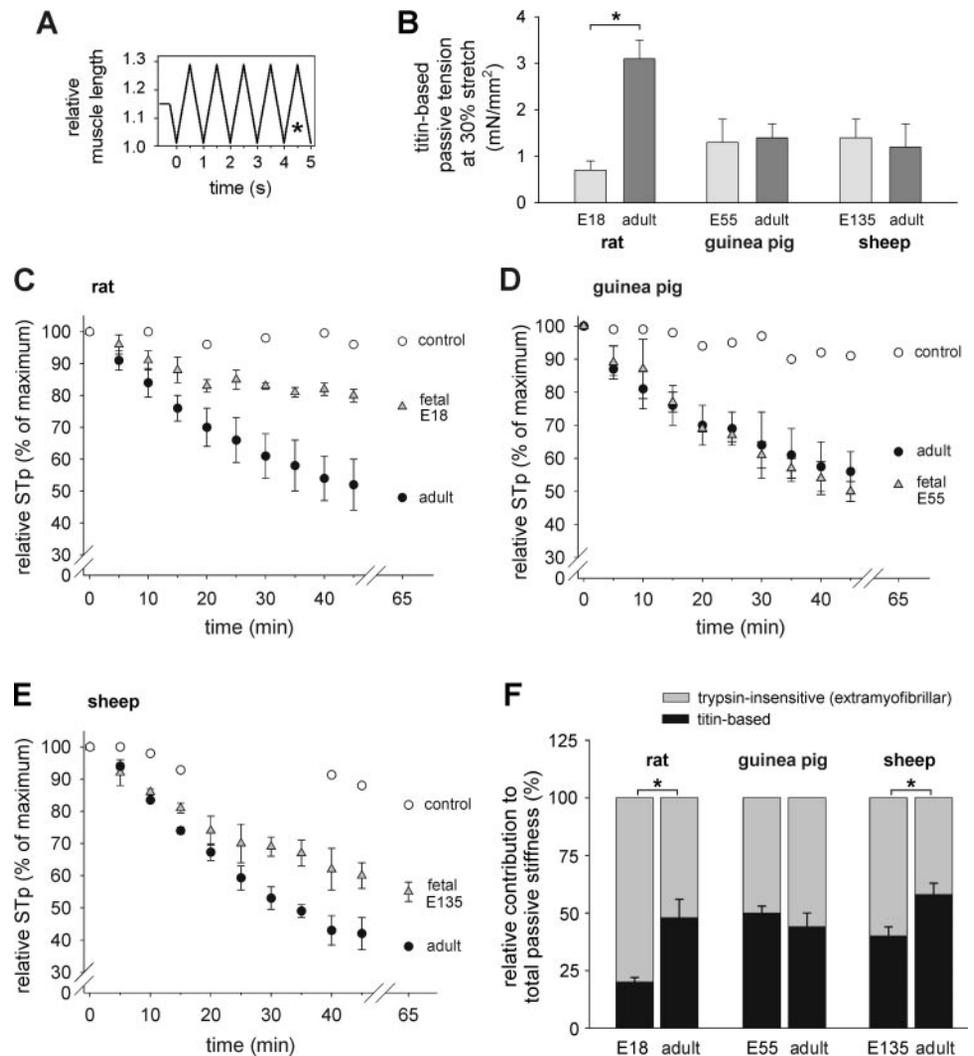
Fig. 3. Passive tension and passive stiffness (ST_p) of skinned cardiac-fiber bundles during stretch-release cycles before and after proteolytic degradation of titin. *A*: experimental protocol. Asterisk denotes the 5th stretch-release cycle, from which passive tension and ST_p were calculated. *B*: titin-borne (trypsin sensitive) passive tension at 30% stretch (means $\pm$ SE, $n = 3$–4 per bar). *C–E*: relative ST_p of fetal and adult fiber bundles from rat, guinea pig, and sheep during 45-min-long treatment with low-dose trypsin. Control = tissue (adult) not treated with trypsin. *F*: relative contribution of titin to total ST_p compared with that of trypsin-insensitive extramyofibrillar structures (e.g., mainly collagen). Values are means $\pm$ SE ($n = 3$–6 per bar). The respective fetal stages are indicated. *$P < 0.05$ in Student's *t*-test.

trypsin treatment leveled out after ~45 min in fetal and adult cardiac fibers of all three species (Fig. 3, *C–E*). Measurements on fibers that had not been treated with trypsin (control) revealed a slight ST_p decrease of no more than 15% during a time period of ~1 h (Fig. 3, *C–E*). This "normal" stiffness decrease was taken into account for the calculation of the trypsin effect. With the disruption of titin, ST_p decreased within 45 min to 40–50% of the level before trypsin application in the adult tissue of all three species (Fig. 3). Also cardiac strips from fetal guinea pig (E55) and lamb (E135) exhibited a substantial reduction in ST_p to ~55% of the value before trypsin treatment (Fig. 3, *D* and *E*). The deduced proportions of titin-based ST_p showed only minor variability, 42–58%, between fetal and adult sheep, fetal and adult guinea pig, and adult rat heart (Fig. 3*F*). A somewhat elevated percentage of titin-borne ST_p was seen in adult sheep compared with fetal lamb ($P = 0.025$ in Student's *t*-test). In contrast, fibers from fetal rat heart (E18) were much less affected by trypsin, and ST_p decreased only to ~80% of the initial value (Fig. 3*C*). Hence, only 20% of the total ST_p was titin-based in fetal rat heart, significantly less ($P < 0.01$ in Student's *t*-test) than in adult rat heart (48%). A summary of results (Fig. 3*F*) shows that the trypsin-insensitive components, most probably the
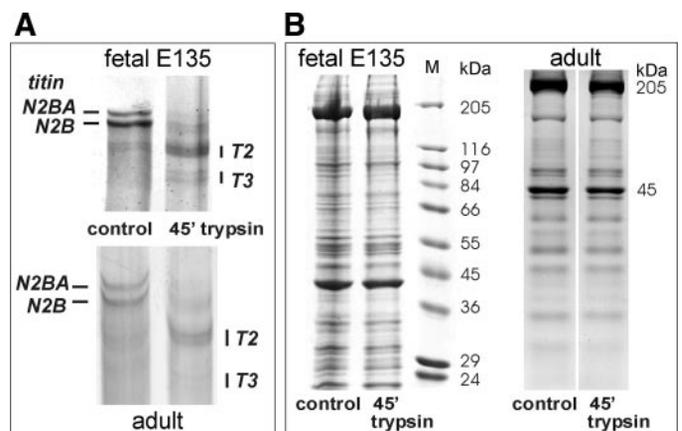

Fig. 4. Impact of trypsin treatment on protein expression. *A*: titin proteolysis detected by 2% SDS-PAGE. Example is shown for skinned cardiac-fiber bundles from fetal (E135) lamb (*top*) and adult sheep (*bottom*). After 45-min trypsin treatment, the titin-degradation bands T2 and T3 appear; essentially no intact titin remains. Coomassie staining. *B*: proteins in the lower-molecular-mass range in skinned fiber bundles from fetal (E135) lamb (*left two lanes*) and adult sheep (*right two lanes*) before and after 45-min-long trypsin treatment. No significant changes of muscle proteins <250 kDa are detectable. Coomassie staining, 12.5% SDS-PAGE.

collagen fibers, contributed between ~40% and ~60% to total ST_p in all tissues at both developmental stages, except in fetal rat heart, where they contributed 80%. Interestingly, the relative importance of titin for total ST_p scaled with the proportion of stiff N2B-titin isoform expressed (compare Fig. 3F and Fig. 2C). A correlation with the titin-isoform composition (Fig. 2C) is also evident for titin-borne PT (Fig. 3B). Analysis of the trypsin-sensitive (=titin-borne) PT level at 30% stretch demonstrated that in guinea pig and sheep, this PT component is independent of the developmental stage, which fits with the similar N2BA:N2B ratios in these species at those stages. In contrast, a large increase in titin-borne PT occurs in rat from

stages E18 to adult (Fig. 3B), consistent with the rise in N2B isoform percentage.

Myocyte ultrastructure, MyHC, and collagen density changes during cardiac development. To gain insights into ultrastructural differences between the tissue types, we prepared electron micrographs of fetal and adult heart samples from rat, guinea pig, and sheep. Figure 5 (main panels) shows representative images. Regular striations indicating well-defined sarcomere structure were only beginning to appear in fetal (E18) rat hearts (Fig. 5A, *left*) but were readily seen in fetal guinea pig (E55) (Fig. 5B, *left*) and sheep (E112) hearts (Fig. 5B, *left*). The abundance and alignment of myofibrils was
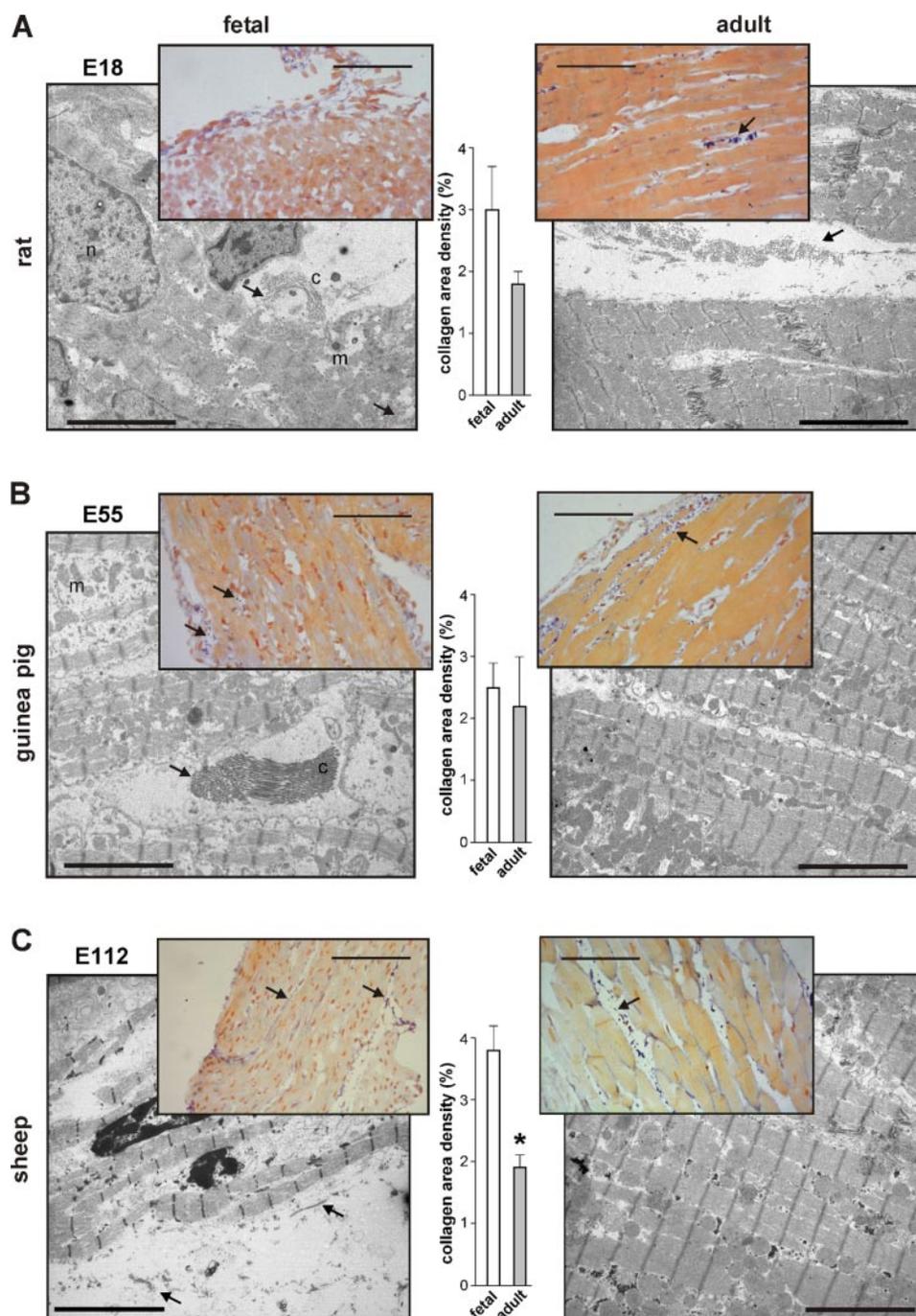

Fig. 5. Myocyte ultrastructure and collagen distribution in heart tissue of fetal (*left*) and adult (*right*) rat (A), guinea pig (B), and sheep (C). Fetal tissue was analyzed at E18 (rat), E55 (guinea pig), and E112 (lamb), respectively. Note clear striation pattern and abundance of myofibrils in fetal guinea pig and sheep in contrast to fetal rat. Collagen depositions (c) on electron micrographs are depicted by arrows; n, nucleus; m, mitochondria; scale bars, 6 μm. *Insets*: histological analysis by Azan staining on semithin sections of fetal and adult fibers to distinguish cardiomyocytes (red-pink) from connective tissue (blue). Scale bars, 100 μm. From these and similar images the average collagen area density was estimated; results are depicted in the graphs (data are means ± SE, $n = 4$ images per group; *$P < 0.05$ in Student's *t*-test).

more similar in fetal and adult hearts of guinea pig or sheep than in those of rat (compare left panels vs. right panels in Fig. 5). Furthermore, the difference in the number of mitochondria was large in fetal compared with adult rat but smaller between fetal and adult guinea pig/sheep (data not shown). In contrast, no obvious differences were detectable between the respective fetal and adult tissues with regard to the appearance of collagen fibers.

To further demonstrate developmental differences in the abundance of myofibrils, we analyzed the MyHC content relative to the total protein content by 10% SDS-PAGE (Table 1). The percentage of MyHC was much lower in E18 rat and E82 sheep hearts than in adult rat and sheep but showed only a minor increase from the fetal to the adult stage in guinea pig hearts. Neonatal (1 day) rat already had a MyHC proportion similar to adult rat, and late-fetal (E135) sheep hearts expressed MyHC at levels intermediate between those of E82 and adult sheep. These results support the notion that fetal (E18) rat hearts are still lacking an abundant myofibrillar network, whereas a relatively high occupancy with myofibrils is characteristic of guinea pig heart tissue already during mid gestation and sheep heart tissue at late-fetal stages.

Azan staining of semithin sections was used to distinguish cardiomyocytes (pink-red) from collageneous tissue (blue) (Fig. 5, *A–C*, insets). Again, the higher degree of tissue organization in adult compared with fetal hearts was particularly obvious for rat. Density calculations of the area occupied by collagen in fetal vs. adult hearts showed differences between species (Fig. 5, *A–C*, graphs). No difference was seen in guinea pig (Fig. 5*B*), whereas the collagen area density tended to be slightly higher in fetal (E18) than in adult rats; however, the difference did not reach statistical significance (Fig. 5*A*). In contrast, collagen occupied twice as much area (~4% vs. ~2%; $P < 0.05$ in Student's *t*-test) in fetal (E112) lambs compared with adult sheep (Fig. 5*C*).

Alterations in isoform expression of TnI and Ca^{2+} sensitivity of force development. Titin-isoform switching during perinatal rat heart development occurs with a similar time course as the isoform shifting of other sarcomere proteins, as shown for TnI (56). A switch in isoform expression during perinatal cardiac development from ssTnI to cTnI has previously been correlated
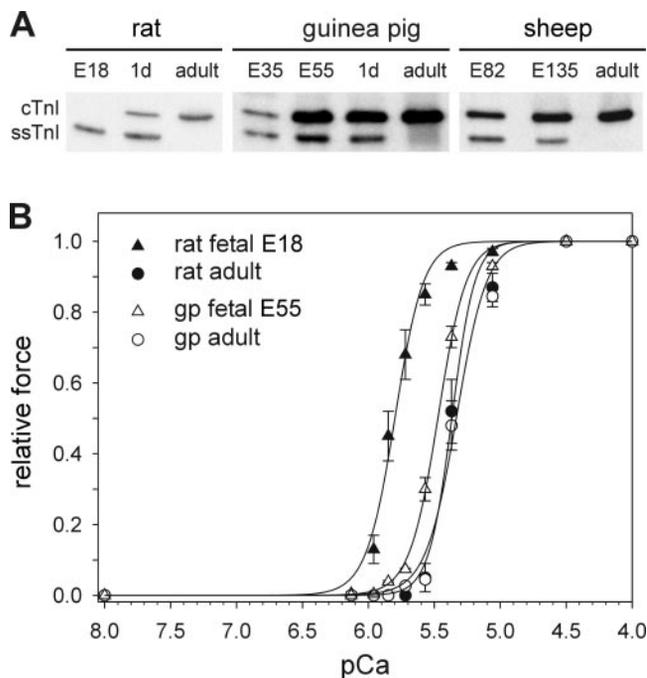

Fig. 6. Developmental changes in troponin-I (TnI) isoform pattern and Ca^{2+} sensitivity of force development. *A*: cardiac (cTnI) and slow skeletal TnI (ssTnI) expression detected by Western blot analysis in late-fetal (E18), neonatal (1 day), and adult rat; in midgestation (E35), late-fetal (E55), neonatal (1 day), and adult guinea pig; and in midgestation (E82), fetal (E135), and adult sheep hearts. *B*: force-pCa-relationships of skinned cardiac fiber bundles from fetal (E18) and adult rats and from fetal (E55) and adult guinea pigs (gp). Force was normalized to F_{max} of each fiber. Data are means ± SE (3–6 fibers per group). Lines indicate best fits using the Hill equation.

to a shift in the Ca^{2+} sensitivity of force generation (16, 46, 53). To test if a switch from ssTnI to cTnI around birth takes place in those hearts that lack a characteristic shift in titin isoforms at that time, we performed Western blot analysis with anti-cTnI antibody (8I-7) on tissue samples from fetal and adult hearts of guinea pig and sheep compared with rat (Fig. 6*A*). Fetal rat hearts (E18) almost exclusively expressed the ssTnI, which was subsequently replaced by cTnI during and after birth, confirming earlier data (56). In contrast, cTnI was strongly expressed in guinea pig hearts at all developmental stages (Fig. 6*A*). At gestational *days E35* and *E55*, cTnI and ssTnI were present in a near-equimolar ratio. In neonatal guinea pig, cTnI was somewhat more prominent than ssTnI, whereas in adult hearts, no ssTnI was detectable. Similar results were obtained for sheep, where both isoforms were expressed in the fetal (E82 and E135) heart and a complete

Table 1. *MyHC content relative to total protein content*

Species/Developmental Stage	MyHC, % of Total Protein
Rat	
E18 (late fetal)	12±1
1 Day	18±0.2
Adult	17±0.3
Guinea pig	
E35 (midgestation)	16±1
E55 (late fetal)	15±3
1 Day	16±2
Adult	19±1.5
Sheep	
E82 (midgestation)	10±1
E135 (late fetal)	14.5±0.5
Adult	19±1

Values are means ± SE; n = 2–3 animals (neonatal guinea pig, n = 1), with 3 gel lanes each. MyHC, myosin heavy chain; E18, E35, E55, E82, and E135 refer to gestational *days 18, 35, 55, 82,* and *135,* respectively; 1 Day refers to neonatal animal 1 day after birth.

Table 2. *Parameters for Ca^{2+} sensitivity of active force development in skinned muscle strips from rat and guinea pig heart*

	pCa50, $-\log[Ca^{2+}]M^{-1}$	Hill Coefficient, n_H
Rat fetus (E18)	5.81±0.03†	6.1±0.3
Rat adult	5.36±0.05	6.2±0.4
Guinea pig fetus (E55)	5.48±0.02*	5.4±0.3
Guinea pig adult	5.34±0.05	4.9±0.9

Values are means ± SE; n = 3–6 per group. *$P < 0.05$, †$P < 0.001$ compared with the adult stage in Student's *t*-test. pCa50, pCa at half-maximum active force level.

replacement of ssTnI by cTnI took place until adulthood (Fig. 6*A*).

To study how the developmental changes in TnI expression alter the Ca^{2+} sensitivity of force development, we measured the force-pCa relationships in skinned cardiac-fiber bundles from fetal and adult rat and guinea pig (Fig. 6*B*). Maximum force development per cross-sectional area was similar in adult rat and fetal (E55) and adult guinea pig but much smaller in fetal (E18) rat hearts (data not shown). Parameters of the Hill fit to the averaged relative force data are shown in Table 2. In the adult tissue of both species, we found no difference in the Ca^{2+} sensitivity of force development, with average pCa_{50} values of 5.34 (guinea pig) and 5.36 (rat). The pCa_{50} of adult guinea pig fibers was lower by 0.14 pCa units ($P < 0.05$ in Student's *t*-test) compared with the fetal (E55) stage. However, the difference was much more pronounced in the rat, in which pCa_{50} was lower by 0.45 pCa units in adult compared with fetal (E18) hearts (Fig. 6*B*). No significant differences in the cooperativity of active force development were observed between fetal and adult fibers from rat or guinea pig, as indicated by the similar Hill coefficients (Table 2).

DISCUSSION

We have analyzed the expression of titin isoforms in LV tissue samples from fetal, newborn, and adult rat, guinea pig, and sheep. As previously described (27, 43, 56), titin in rat hearts switched from larger and more compliant N2BA isoforms in the fetus and neonate to the shorter and stiffer N2B isoform, which is the predominant isoform during adulthood, replacing N2BA-titin almost completely. Elsewhere we speculated (41, 43) that large cardiac N2BA isoforms in the fetus may be needed to keep titin-based PT low during fetal development when the compliance of the heart is restricted by extracardiac constraint (19). Myocardial passive stiffening at around the time of birth could be useful to balance the reduced extracardiac constraint at birth (19) and counteract the increased inflow of blood associated with the suddenly higher power requirements of the newborn heart (43). We now report that this kind of perinatal titin-isoform shift does not occur in the hearts of the nidifugous guinea pig and sheep, in which the compliant fetal N2BA isoforms are partly replaced by the stiffer N2B isoform already during earlier fetal stages. We now propose that the event of birth is not the critical trigger for the titin-isoform shift during cardiac development. Rather, species-specific factors and genetic programming most probably cause large interspecies variability in the time course of developmental titin-isoform transitions.

In mice and rats with a gestation period of ~3 wk, it takes only 2 wk from the time of conception to complete cardiac septation (the remodeling of the heart from a single-channel pump to a dual-channel, synchronously contracting device). Before birth, the rat/mouse fetus has very little time to complete the development of essential organs, and in the early neonates, major developmental transitions are still in progress (58). A different scenario holds true for the nest quitters, guinea pig and sheep, where pregnancy lasts 65–68 and ~150 days, respectively, and where ultrastructure and contractile properties of the late-embryonic heart are already more similar to those of the adult heart (2, 14). Another animal in which cardiac titin-isoform changes have been studied, the pig (27,

41), has a gestation period of ~4 mo (shorter than the 5 mo of sheep) and is a secondary altricial mammal still deaf and blind at birth. Titin-isoform analyses in pig hearts suggested there is a single large isoform of the N2BA type expressed several weeks before birth (41), which is gradually replaced by smaller-size N2BA isoforms and a high proportion of N2B-titin around the time of birth and thereafter (27, 41). This kind of perinatal titin-isoform switching resembles that of rat and mouse heart, although the sequence of transitions is slowed down. Taken together with the present results, it is not unreasonable to assume a more general scenario in which mammals that are still helpless at the time of birth do switch their titin isoforms at approximately the time of birth. In contrast, mammals developing to near the weaning stage before birth show little or no perinatal titin-isoform shift; such a shift may occur much earlier during gestation.

Although we have demonstrated here that a cardiac titin-isoform shift toward increased proportions of N2B takes place during midgestation in sheep and guinea pig, it remains to be seen whether this switch begins with a unique N2BA isoform and no N2B, as in rat heart (43, 56), or whether there is always some percentage of N2B isoform present. Our data suggest that the starting point for the switch in the nest-quitter species is during the first half of the gestation period. Finding out how early the switching begins remains to be studied in future investigations.

Evidence from previous studies suggests that in rats, fetal cardiac sarcomeres are much more compliant than adult sarcomeres, which is consistent with the predominant expression of large N2BA isoforms in fetal hearts and short, stiff N2B-titin in adult hearts (43, 56). Owing to their switch toward higher N2B-titin proportions, the myocardium of pigs also stiffens from the neonatal (1 day) to the adult stage (27, 41, 43). Here, sheep and guinea pig hearts showed very little or no titin-isoform transition during the perinatal period (Fig. 2), and, consequently, titin-borne PT was similar in these species before and after birth (Fig. 3*B*).

We also investigated by using selective titin degradation whether titin's relative importance for passive myocardial stiffness, ST_P, varies during heart development (Fig. 3). Titin contributed to a similar degree to total ST_P in fetal (E55) and adult guinea pig hearts. In sheep hearts, the proportion of titin-based ST_P increased by a mere 15% from the fetal (E135) to the adult stage, concomitant with the ~15% increase in N2B-titin percentage. The largest rise in relative titin stiffness was seen in rat hearts, from 20% in the fetus (E18) to ~50% in the adult, demonstrating a much-increased importance of titin for total ST_P after birth. Electron micrographs of fetal (E18) rat hearts showed immature and scarce myofibrils, whereas fetal (E112) sheep and fetal (E55) guinea pig hearts contained well-structured myocytes with abundant myofibrils (Fig. 5). Also the results of our analysis of the relative MyHC content (Table 1) supported the notion that late-fetal sheep hearts or guinea pig hearts at midgestation already contain an abundant myofibrillar network that is still about to be formed in fetal (E18) rat hearts. Incomplete myofibrillogenesis in fetal rat hearts may add to the low proportion of titin-based stiffness in this tissue type because relatively fewer titin springs per cross-sectional area exist than in fetal sheep and guinea pig hearts, which contain larger numbers of well-developed sarcomeres. In summary, this work suggests two likely reasons for

the great variability in the relative contribution of titin to myocardial ST_p: *1)* there are large interspecies and developmental differences in titin-isoform ratios, and *2)* myofibrillar density and assembly status differ in fetal cardiomyocytes of different species.

The proportion of ST_p that was not due to titin most probably was borne out mainly by the collagen fibers (27, 33, 45). Collagen deposits on electron micrographs appeared to be equally abundant in fetal and adult hearts of the three species, but histological analysis revealed a developmental stage-dependent difference in the collagen area density of sheep hearts only (Fig. 5). Collagen occupied two times larger an area on tissue sections from fetal (E112) lamb compared with those from adult sheep. Interestingly, the fetal lamb heart has long been considered to be stiffer than the adult sheep heart (3, 48, 49). These findings, however, cannot be explained by titin-isoform shifts, as the minor developmental changes in titin expression in sheep hearts (Fig. 2*C*) in fact would cause a small degree of postnatal tissue stiffening. Taken together, we propose that a decreased collagen area density in adult compared with fetal hearts may play a major role in the postnatal passive-stiffness drop in sheep hearts. If so, the collagen-related stiffness changes would counteract the changes in titin-based stiffness during sheep-heart development—a scenario that bears similarly to the situation in end-stage failing human hearts, which are globally stiffened by fibrosis but show reduced ST_p of the myofibrils (33, 39). Possibly, titin-based and collagen-based stiffness counterbalance one another in a coordinated fashion during cardiac development.

During perinatal cardiac development, several sarcomere proteins exhibit isoform switching, and these transitions have often been associated with marked changes in functional properties (10, 32, 46, 53). One of the most pronounced and best-characterized functional adaptations of this kind is altered Ca^{2+} homeostasis. Excitation-contraction coupling is still evolving during perinatal development, and key mechanisms such as the Ca^{2+}-induced Ca^{2+}-release are not yet fully established in late-fetal rat cardiomyocytes (12, 34). Altered Ca^{2+} homeostasis is believed to lead to reduced intracellular Ca^{2+} concentration, which can be partly compensated for in the fetal heart by increased Ca^{2+} sensitivity of myofibrillar force development. As a key player in defining embryonic Ca^{2+} sensitivity, various studies have identified the regulatory protein subunit TnI (35–37, 46, 53, 55). In the LVs of fetal rats and mice, the slow skeletal TnI isoform is expressed, which is then replaced by the cardiac cTnI isoform within the first days after birth (7, 15, 18, 50, 52, 53, 56). The isoforms of TnT also affect the Ca^{2+} sensitivity (8). However, although there is a shift of cardiac TnT isoforms during the perinatal period in mouse heart, a recent study confirmed the pivotal role of the ssTnI-cTnI switching in defining myofilament Ca^{2+} sensitivity (17). As soon as the expression of cTnI is initiated, a reduction in Ca^{2+} sensitivity can be observed. Because the cTnI first appears in newborn rat hearts at about the same time as N2B titin (56), we decided to study TnI-isoform expression also in developing guinea pig and sheep hearts, which almost entirely lack a perinatal titin-isoform switch. In these two species the adult cTnI isoform was coexpressed along with the ssTnI isoform already well before birth (Fig. 6*A*). This reflects the situation in fetal human hearts, where the transition from ssTnI to cTnI expression begins already after 20–33 wk of gestation

(7). Thus, also in terms of TnI expression, the fetal hearts of guinea pig and sheep are more similar to their adult counterparts than the fetal rat heart is to the adult rat heart.

By measuring the Ca^{2+} sensitivity of force development in skinned cardiac fiber bundles, we confirmed the marked decrease by ~0.45 pCa units that has previously been reported for adult compared with fetal rat hearts (35, 46). The perinatal decrease in Ca^{2+} sensitivity was much smaller, 0.14 pCa units, in fibers from guinea pig, in which cTnI and ssTnI are coexpressed before birth. In this nest-quitter species, the developmental transition in Ca^{2+} sensitivity apparently was nearly completed already before birth.

One can speculate that the coordinated developmental changes in TnI and titin isoform expression, ST_p, and Ca^{2+} sensitivity depend on common intracellular or extracellular signals that trigger a timed transition in many proteins and diverse functional properties. As yet, the presence of such possible trigger(s) remains obscure. Several reports revealed a crucial role for thyroid hormone in regulating TnI-isoform expression in developing rat ventricles and tissue cultures (6, 11). Thyroid hormone influences cTnI expression mainly in postnatal and young adult rats, and hypothyroidism can be associated with a delay in TnI-isoform switching (6, 11). In other studies, thyroid hormone was shown to inhibit slow skeletal TnI expression in myocardial cells of a murine cTnI-null model (23, 47). Whether upregulation of thyroid hormone during fetal development also contributes to the mechanisms that regulate the expression pattern of titin isoforms remains to be seen. This work, however, suggests that the event of birth is not the critical trigger for perinatal TnI and titin isoform shifts and related functional transitions. Future studies need to unravel the complex mechanisms that tightly regulate protein expression and adaptation of passive and active properties during development in a species-specific manner.

REFERENCES

1. **Agarkova I, Auerbach D, Ehler E, and Perriard JC.** A novel marker for vertebrate embryonic heart, the EH-myomesin isoform. *J Biol Chem* 275: 10256–10264, 2000.
2. **Agata N, Tanaka H, and Shigenobu K.** Inotropic effects of ryanodine and nicardipine on fetal, neonatal and adult guinea-pig myocardium. *Eur J Pharmacol* 260: 47–55, 1994.
3. **Anderson PA, Glick KL, Manring A, and Crenshaw C Jr.** Developmental changes in cardiac contractility in fetal and postnatal sheep: in vitro and in vivo. *Am J Physiol Heart Circ Physiol* 247: H371–H379, 1984.
4. **Anderson PA, Manring A, Glick KL, and Crenshaw CC Jr.** Biophysics of the developing heart. III. A comparison of the left ventricular dynamics of the fetal and neonatal lamb heart. *Am J Obstet Gynecol* 143: 195–203, 1982.
5. **Ausoni S, De Nardi C, Moretti P, Gorza L, and Schiaffino S.** Developmental expression of rat cardiac troponin I mRNA. *Development* 112: 1041–1051, 1991.
6. **Averyhart-Fullard V, Fraker LD, Murphy AM, and Solaro RJ.** Differential regulation of slow-skeletal and cardiac troponin I mRNA during

development and by thyroid hormone in rat heart. *J Mol Cell Cardiol* 26: 609–616, 1994.

7. **Bhavsar PK, Dhoot GK, Cumming DV, Butler-Browne GS, Yacoub MH, and Barton PJ.** Developmental expression of troponin I isoforms in fetal human heart. *FEBS Lett* 292: 5–8, 1991.

8. **Brotto MA, Biesiadecki BJ, Brotto LS, Nosek TM, and Jin JP.** Coupled expression of troponin T and troponin I isoforms in single skeletal muscle fibers correlates with contractility. *Am J Physiol Cell Physiol* 290: C567–C576, 2006.

9. **Cappelli V, Bottinelli R, Poggesi C, Moggio R, and Reggiani C.** Shortening velocity and myosin and myofibrillar ATPase activity related to myosin isoenzyme composition during postnatal development in rat myocardium. *Circ Res* 65: 446–457, 1989.

10. **Carrier L, Boheler KR, Chassagne C, de la Bastie D, Wisnewsky C, Lakatta EG, and Schwartz K.** Expression of the sarcomeric actin isogenes in the rat heart with development and senescence. *Circ Res* 70: 999–1005, 1992.

11. **Dieckman LJ and Solaro RJ.** Effect of thyroid status on thin-filament Ca^{2+} regulation and expression of troponin I in perinatal and adult rat hearts. *Circ Res* 67: 344–351, 1990.

12. **Fabiato A and Fabiato F.** Calcium-induced release of calcium from the sarcoplasmic reticulum of skinned cells from adult human, dog, cat, rabbit, rat, and frog hearts and from fetal and new-born rat ventricles. *Ann NY Acad Sci* 307: 491–522, 1978.

13. **Freiburg A, Trombitas K, Hell W, Cazorla O, Fougerousse F, Centner T, Kolmerer B, Witt C, Beckmann JS, Gregorio CC, Granzier H, and Labeit S.** Series of exon-skipping events in the elastic spring region of titin as the structural basis for myofibrillar elastic diversity. *Circ Res* 86: 1114–1121, 2000.

14. **Friedman WF and Kirkpatrick SE.** In situ physiological study of the developing heart. *Recent Adv Stud Card Struct Metab* 5: 497–504, 1975.

15. **Gao L, Kennedy JM, and Solaro RJ.** Differential expression of TnI and TnT isoforms in rabbit heart during the perinatal period and during cardiovascular stress. *J Mol Cell Cardiol* 27: 541–550, 1995.

16. **Godt RE, Fogaca RT, and Nosek TM.** Changes in force and calcium sensitivity in the developing avian heart. *Can J Physiol Pharmacol* 69: 1692–1697, 1991.

17. **Gomes AV, Venkatraman G, Davis JP, Tikonuva SB, Engel P, Solaro RJ, and Potter JD.** Cardiac troponin T isoforms affect the Ca^{2+}-sensitivity of force development in the presence of slow skeletal troponin I. *J Biol Chem* 279: 49579–49587, 2004.

18. **Gorza L, Ausoni S, Merciai N, Hastings KE, and Schiaffino S.** Regional differences in troponin I isoform switching during rat heart development. *Dev Biol* 156: 253–264, 1993.

19. **Grant DA, Fauchere JC, Eede KJ, Tyberg JV, and Walker AM.** Left ventricular stroke volume in the fetal sheep is limited by extracardiac constraint and arterial pressure. *J Physiol* 535: 231–239, 2001.

20. **Granzier H and Labeit S.** Cardiac titin: an adjustable multi-functional spring. *J Physiol* 541: 335–342, 2002.

21. **Hirakow R and Gotoh T.** Quantitative studies on the ultrastructural differentiation and growth of mammalian cardiac muscle cells. II. The atria and ventricles of the guinea pig. *Acta Anat (Basel)* 108: 230–237, 1980.

22. **Hoh JF, McGrath PA, and Hale PT.** Electrophoretic analysis of multiple forms of rat cardiac myosin: effects of hypophysectomy and thyroxine replacement. *J Mol Cell Cardiol* 10: 1053–1076, 1978.

23. **Huang X, Lee KJ, Riedel B, Zhang C, Lemanski LF, and Walker JW.** Thyroid hormone regulates slow skeletal troponin I gene inactivation in cardiac troponin I null mouse hearts. *J Mol Cell Cardiol* 32: 2221–2228, 2000.

24. **Hunkeler NM, Kullman J, and Murphy AM.** Troponin I isoform expression in human heart. *Circ Res* 69: 1409–1414, 1991.

25. **Kaiser S, Kruijver FP, Swaab DF, and Sachser N.** Early social stress in female guinea pigs induces a masculinization of adult behavior and corresponding changes in brain and neuroendocrine function. *Behav Brain Res* 144:199–210, 2003.

26. **Kirkpatrick SE, Covell JW, and Friedman WF.** A new technique for the continuous assessment of fetal and neonatal heart performance. *Am J Obstet Gynecol* 116: 963–972, 1973.

27. **Lahmers S, Wu Y, Call DR, Labeit S, and Granzier H.** Developmental control of titin isoform expression and passive stiffness in fetal and neonatal myocardium. *Circ Res* 94: 505–513, 2004.

28. **Li H, Linke WA, Oberhauser AF, Carrion-Vazquez M, Kerkvliet JG, Lu H, Marszalek PE, and Fernandez JM.** Reverse engineering of the giant muscle protein titin. *Nature* 418: 998–1002, 2002.

29. **Linke WA and Fernandez JM.** Cardiac titin: Molecular basis of elasticity and cellular contribution to elastic and viscous stiffness components in myocardium. *J Muscle Res Cell Motil* 23: 483–497, 2002.

30. **Linke WA, Ivemeyer M, Labeit S, Hinssen H, Ruegg JC, and Gautel M.** Actin-titin interaction in cardiac myofibrils: probing a physiological role. *Biophys J* 73: 905–919, 1997.

31. **Linke WA, Rudy DE, Centner T, Gautel M, Witt C, Labeit S, and Gregorio CC.** I-band titin in cardiac muscle is a three-element molecular spring and is critical for maintaining thin filament structure. *J Cell Biol* 146: 631–644, 1999.

32. **Lompre AM, Nadal-Ginard B, and Mahdavi V.** Expression of the cardiac ventricular α- and β-myosin heavy chain genes is developmentally and hormonally regulated. *J Biol Chem* 259: 6437–6446, 1984.

33. **Makarenko I, Opitz CA, Leake MC, Neagoe C, Kulke M, Gwathmey JK, del Monte F, Hajjar RJ, and Linke WA.** Passive stiffness changes caused by upregulation of compliant titin isoforms in human dilated cardiomyopathy hearts. *Circ Res* 95: 708–716, 2004.

34. **Marsh JD and Allen PD.** Developmental regulation of cardiac calcium channels and contractile sensitivity to [Ca]ₒ. *Am J Physiol Heart Circ Physiol* 256: H179–H185, 1989.

35. **Martin AF, Ball K, Gao LZ, Kumar P, and Solaro RJ.** Identification and functional significance of troponin I isoforms in neonatal rat heart myofibrils. *Circ Res* 69: 1244–1252, 1991.

36. **Metzger JM, Michele DE, Rust EM, Borton AR, and Westfall MV.** Sarcomere thin filament regulatory isoforms. Evidence of a dominant effect of slow skeletal troponin I on cardiac contraction. *J Biol Chem* 278: 13118–13123, 2003.

37. **Morimoto S and Goto T.** Role of troponin I isoform switching in determining the pH sensitivity of Ca^{2+} regulation in developing rabbit cardiac muscle. *Biochem Biophys Res Commun* 267: 912–917, 2000.

38. **Nagueh SF, Shah G, Wu Y, Torre-Amione G, King NM, Lahmers S, Witt CC, Becker K, Labeit S, and Granzier HL.** Altered titin expression, myocardial stiffness, and left ventricular function in patients with dilated cardiomyopathy. *Circulation* 110: 155–162, 2004.

39. **Neagoe C, Kulke M, del Monte F, Gwathmey JK, de Tombe PP, Hajjar RJ, and Linke WA.** Titin isoform switch in ischemic human heart disease. *Circulation* 106: 1333–1341, 2002.

40. **Neagoe C, Opitz CA, Makarenko I, and Linke WA.** Gigantic variety: expression patterns of titin isoforms in striated muscles and consequences for myofibrillar passive stiffness. *J Muscle Res Cell Motil* 24: 175–189, 2003.

41. **Opitz CA and Linke WA.** Plasticity of cardiac titin/connectin in heart development. *J Muscle Res Cell Motil* February 08, 2006; doi:10.1007/s10974–005-9040–7.

42. **Opitz CA, Kulke M, Leake MC, Neagoe C, Hinssen H, Hajjar RJ, and Linke WA.** Damped elastic recoil of the titin spring in myofibrils of human myocardium. *Proc Natl Acad Sci USA* 100: 12688–12693, 2003.

43. **Opitz CA, Leake MC, Makarenko I, Benes V, and Linke WA.** Developmentally regulated switching of titin size alters myofibrillar stiffness in the perinatal heart. *Circ Res* 94: 967–975, 2004.

44. **Phoon CK.** Circulatory physiology in the developing embryo. *Curr Opin Pediatr* 13: 456–464, 2001.

45. **Prado LG, Makarenko I, Andresen C, Kruger M, Opitz CA, and Linke WA.** Isoform diversity of giant proteins in relation to passive and active contractile properties of rabbit skeletal muscles. *J Gen Physiol* 126: 461–480, 2005.

46. **Reiser PJ, Westfall MV, Schiaffino S, and Solaro RJ.** Tension production and thin-filament protein isoforms in developing rat myocardium. *Am J Physiol Heart Circ Physiol* 267: H1589–H1596, 1994.

47. **Riedel B, Jia Y, Du J, Akerman S, and Huang X.** Thyroid hormone inhibits slow skeletal TnI expression in cardiac TnI-null myocardial cells. *Tissue Cell* 37: 47–51, 2005.

48. **Romero T and Friedman WF.** Limited left ventricular response to volume overload in the neonatal period: a comparative study with the adult animal. *Pediatr Res* 13: 910–915, 1979.

49. **Romero T, Covell J, and Friedman WF.** A comparison of pressure-volume relations of the fetal, newborn, and adult heart. *Am J Physiol* 222: 1285–1290, 1972.

50. **Sabry MA and Dhoot GK.** Identification and pattern of expression of a developmental isoform of troponin I in chicken and rat cardiac muscle. *J Muscle Res Cell Motil* 10: 85–91, 1989.

51. **Saggin L, Ausoni S, Gorza L, Sartore S, and Schiaffino S.** Troponin T switching in the developing rat heart. *J Biol Chem* 263: 18488–18492, 1988.

52. **Saggin L, Gorza L, Ausoni S, and Schiaffino S.** Troponin I switching in the developing heart. *J Biol Chem* 264: 16299–16302, 1989.

53. **Siedner S, Kruger M, Schroeter M, Metzler D, Roell W, Fleischmann BK, Hescheler J, Pfitzer G, and Stehle R.** Developmental changes in contractility and sarcomeric proteins from the early embryonic to the adult stage in the mouse heart. *J Physiol* 548: 493–505, 2003.

54. **Smolich JJ, Walker AM, Campbell GR, and Adamson TM.** Left and right ventricular myocardial morphometry in fetal, neonatal, and adult sheep. *Am J Physiol Heart Circ Physiol* 257: H1–H9, 1989.

55. **Solaro RJ, Lee JA, Kentish JC, and Allen DG.** Effects of acidosis on ventricular muscle from adult and neonatal rats. *Circ Res* 63: 779–787, 1988.

56. **Warren CM, Krzesinski PR, Campbell KS, Moss RL, and Greaser ML.** Titin isoform changes in rat myocardium during development. *Mech Dev* 121: 1301–1312, 2004.

57. **Warren CM, Krzesinski PR, and Greaser ML.** Vertical agarose gel electrophoresis and electroblotting of high-molecular-weight proteins. *Electrophoresis* 24: 1695–1702, 2003.

58. **Wessels A and Sedmera D.** Developmental anatomy of the heart: a tale of mice and man. *Physiol Genomics* 15: 165–176, 2003.

59. **Westfall MV and Solaro RJ.** Alterations in myofibrillar function and protein profiles after complete global ischemia in rat hearts. *Circ Res* 70: 302–313, 1992.

60. **Whalen RG and Sell SM.** Myosin from fetal hearts contains the skeletal muscle embryonic light chain. *Nature* 286: 731–733, 1980.

61. **Wu Y, Cazorla O, Labeit D, Labeit S, and Granzier H.** Changes in titin and collagen underlie diastolic stiffness diversity of cardiac muscle. *J Mol Cell Cardiol* 32: 2151–2162, 2000.